ChemSusChem

Chemistry–Sustainability–Energy–Materials

Chemistry Europe

European Chemical Societies Publishing

Accepted Article

Title: Unveiling the modifications of biomass polysaccharides during thermal treatment in cholinium chloride:lactic acid deep eutectic solvent

Authors: Eduarda S. Morais, André Miguel da Costa Lopes, Mara G. Freire, Carmen S. R. Freire, and Armando J. D. Silvestre

To be cited as: *ChemSusChem* 10.1002/cssc.202002301

Link to VoR: https://doi.org/10.1002/cssc.202002301

WILEY-VCH

10.1002/cssc.202002301

Unveiling the modifications of biomass polysaccharides during thermal treatment in cholinium chloride:lactic acid deep eutectic solvent

Eduarda S. Morais, Dr. André M. da Costa Lopes, Dr. Mara G. Freire, Dr. Carmen S. R. Freire and Prof. Armando J. D. Silvestre*

CICECO—Aveiro Institute of Materials, Department of Chemistry, University of Aveiro, 3810-193 Aveiro, Portugal

*Corresponding author: andremcl@ua.pt

Table of Contents

An in-depth investigation of the thermal treatment of biomass polysaccharides with [Ch]Cl:LA (1:10) deep eutectic solvent allowed the identification of relevant physicochemical and morphological modifications of polysaccharides, such as cellulose fiber shortening, cellulose esterification, lactic acid grafting from xylan, among others. The degradation of [Ch]Cl:LA (1:10) at prolonged treatment was also observed.

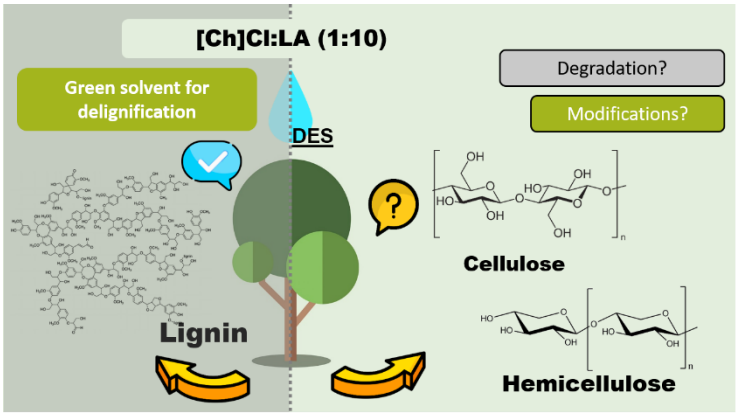

Abstract

A deep analysis upon the chemical modifications of the cellulose and hemicelluloses fractions that take place during biomass delignification with deep eutectic solvents (DES) is lacking in literature, being this a critical issue given the continued research on DES for this purpose. This work intends to fill this gap by disclosing a comprehensive study on the chemical modifications of cellulose (microcrystalline cellulose and bleached kraft pulp) and hemicelluloses (xylans) during thermal treatment (130 °C) with cholinium chloride:lactic acid ([Ch]Cl:LA) at molar ratio 1:10, one of the best reported DES for biomass delignification. The obtained data revealed that [Ch]Cl:LA (1:10) has a negative impact on the polysaccharides fractions at prolonged treatments (>4 h), resulting on substantial modifications including the esterification of cellulose with lactic acid, shortening of fibers length, fibers agglomeration and side reactions of the hemicelluloses fraction (*e.g.* humin formation, lactic acid grafting). Wood delignification trials with [Ch]Cl:LA (1:10) at the same conditions also corroborate these findings. Moreover, the DES suffers degradation, including the formation of lactic acid derivatives and its polymerization. Therefore, short time delignification treatments are strongly recommended when using the [Ch]Cl:LA DES, so that a sustainable fractionation of biomass into high quality cellulose fibers, isolated lignin, and xylose/furfural co-production along with solvent recyclability could be achieved.

Keywords. Biomass, deep eutectic solvents, green chemistry, polysaccharides, solvent stability

1. Introduction

Vegetal biomass is an abundant renewable resource that is a versatile feedstock for the sustainable production of energy, fuels, chemicals and materials, embedded in the bioeconomy strategy proposed by the European Commission.[1,2] The processing of plant biomass is thus a response to the excessive use of pollutant and non-renewable fossil resources that are largely responsible for the current climatic and pollution scenarios.[2] The sustainable exploitation of biomass should rely in the complete fractionation and cascade conversion of its components through physical, chemical, thermochemical and biochemical processing platforms, synergistically employed in biorefinery infrastructures.[3,4] In this context, fractionation efficiency must be seen as one of the top priorities in the evaluation of innovative technologies envisioning high sustainability in biomass valorization. Furthermore, the environmental footprint of these technologies is also a target of critical attention.[1,5]

Lignocellulosic resources, including wood, energy crops, agriculture and forestry residues represent a major part of plant-derived biomass feedstocks, being mainly composed of cellulose, hemicelluloses and lignin.[6] Cellulose is a semi-crystalline linear homopolysaccharide constituted solely by glucose units linked together through β-(1,4)-glycosidic bonds,[7] whereas hemicelluloses are a group of amorphous and branched heteropolysaccharides composed of different monosaccharides (*e.g.* xylose, arabinose, mannose, fructose, etc.) and uronic acids, and are generally acetylated.[6] Xylans composed of xylose, as main monosaccharide, are one of the major examples. On the other hand, lignin is formed by phenylpropanoid units randomly linked by C-C and C-O covalent bonds forming an aromatic matrix.[8] The strong intra- and interlinkages existing between lignin and polysaccharides make of lignocellulosic biomass a very recalcitrant material,

and thus, achieving an effective biomass fractionation is a key challenge for the development of a biobased economy.[9]

Currently, cellulose is still widely processed into paper and cardboard products by pulp and paper industries, whereas novel cellulose-based materials (e.g. composites, nanomaterials, among others) have been purposed as renewable alternatives for the future.[10–13] Moreover, cellulose can be chemically or biotechnologically converted into biofuels (e.g. ethanol and butanol)[6,14] and added-value products (e.g. hydroxymethylfurfural and levulinic acid).[15] In the case of hemicelluloses, other valorization approaches can be adopted. For instance, xylans can be depolymerized into xylose, which in turn can be converted into platform chemicals, such as furfural and xylitol.[16–18]

The most common way to obtain biomass polysaccharides is to remove lignin through delignification processes. For instance, pulp and paper industries use Kraft and Soda processes for an efficient wood delignification to produce high quality cellulose fibers.[19] Other technologies like organosolv and hydrothermal treatments have been also applied to delignify different types of biomass,[20,21] leaving the polysaccharides fraction accessible for further conversion into added-value products. However, those processes use non-benign solvents and reagents, and are highly energy intensive.[20] Furthermore, some of those processes lack fractionation efficiency by degrading or producing low-quality fractions of lignin and hemicelluloses, compromising the objective to accomplish efficient, selective and sustainable biomass processing. In this sense, innovative processes have been chased, wherein the application of green solvents has been addressed as an alternative strategy.[22]

In the past years, an ultimate class of green solvents called Deep Eutectic Solvents (DES) has been attracting significant interest amongst academia and industry. DES are mixtures of at least

two components, a hydrogen bond acceptor (HBA) and a hydrogen bond donor (HBD) that establish strong hydrogen-bonding interactions, providing a significant depression of the mixture's melting temperature (deviating from the ideal behavior) in comparison to those of the individual components.[23] This phenomenon allows some mixtures to be liquid at room temperature and to be used as solvents in a myriad of applications.[24] One of the most promising approaches that has been proposed as a future low-carbon technology is the biomass valorization assisted by these solvents.[22] One of the main successful examples lies in the application of acidic DES for biomass delignification.[25,26]

Among several acidic DES, cholinium chloride:lactic acid ([Ch]Cl:LA) has demonstrated excellent efficiency on lignin dissolution[27,28] and has been placed as one of the best performance DES for biomass delignification.[25,26,29–31] This DES is able to dissolve up to 11.82 wt.% lignin (96% alkali lignin, low sulfonate content) at 60 ˚C, while negligible or no cellulose dissolution was perceived under the studied conditions.[27] As consequence of its selectivity for lignin solubilization, this system has been applied in biomass delignification, as demonstrated by Alvarez-Vasco *et al.*[25] and Shen *et al*.[26] Other works have also reported a successful removal of lignin (60.0 – 93.1 wt.%) from different biomass sources using [Ch]Cl:LA.[29,30,32] This DES was referred to selectively cleave β-O-4 ether linkages in lignin, which facilitates its extraction from biomass.[25] Moreover, the study of the molar ratio between [Ch]Cl and LA showed that a high molar ratio of LA (*e.g.* 1:5, 1:10 and 1:15)[26,27,29,30] favors delignification. It was, however, demonstrated that [Ch]Cl plays an essential role even at low contents as it brings a positive impact on delignification when contrasting to pure lactic acid.[33] This effect was recently explained by a nucleophile substitution of lignin hydroxyl groups by chloride anions, allowing the formation of stable intermediates that favor lignin ether bond cleavage.[34]

After processing lignocellulosic biomass with [Ch]Cl:LA, a cellulose-rich pulp as solid fraction and a DES liquid stream with dissolved lignin are produced.[25,29,31] Subsequently, lignin can be easily precipitated from the liquid stream by dilution with water, which acts as lignin anti-solvent.[25] The precipitated lignin has been characterized by different spectroscopic techniques and commonly highlighted as a high-quality fraction. High purity, ranging from 85 wt.% to 95 wt.%, has been reported for these lignins and their use in further applications have been recommended.[25,26,29] Furthermore, [Ch]Cl:LA extracted lignins are sulphur- and carbohydrate-free and show low condensation degree and homogeneous molecular size distribution.[25,26,29]

Despite the efficient delignification achieved with [Ch]Cl:LA, the characterization of isolated cellulose fibers has not been fully addressed. Additionally, scarce attention has been given to the fate of hemicelluloses during biomass treatment with this DES, which can be considered of utmost importance for their subsequent valorization. Furthermore, it has been reported that xylans' structure is maintained in neutral to mild alkaline-based DES, such as [Ch]Cl:Urea,[35] while in the presence of acidic [Ch]Cl-based DES, comprising oxalic, malic or glycolic acids, xylans are hydrolyzed and favorably converted into furfural.[18,36]

Based on the strong potential of the [Ch]Cl:LA DES to process lignocellulosic biomass, while foreseeing its large-scale application, the present work aims at providing deep insights on the influence of [Ch]Cl:LA (at the molar ratio 1:10) on the chemical structure of polysaccharides representative biomass (*viz.* cellulose and xylans since these fractions are the most desired for further processing) during thermal treatment, mimicking delignification conditions. The modification, depolymerization and degradation of these polysaccharides over time were addressed for a better understanding of the chemical reactions taking place during biomass processing. The occurrence of those phenomena in real wood delignification processes was also

accessed with *Eucalyptus globulus* wood. At last, the stability of the solvent was studied envisaging its recyclability.

2. Experimental

2.1. Chemicals and materials

Cholinium chloride ([Ch]Cl) (≥ 99% purity) and DL-lactic acid (LA) (≥ 85 % purity), both supplied by Sigma (USA), were used as HBD and HBA, respectively. Xylose (≥ 99 % purity) was supplied by Merck (Germany) and furfural (≥ 99 % purity) by Sigma (USA). Commercial beechwood xylan (9.39 wt.% humidity) from Apolo Scientific (UK) and Avicel® microcrystalline cellulose (MCC) PH 101 (3.61 wt.% humidity) with ≈100 μm particle size were purchased from Sigma. Both cellulose diacetate (DE = 2) and cellulose triacetate Selectophore^{TM} (DE = 2) were purchased from Sigma (USA).

Bleached kraft pulp (BKP) (6.82 wt.% humidity) and milled *Eucalyptus globulus* wood (< 40 mesh) composed of approximately 50, 14 and 20 wt% of cellulose, xylans and lignin, respectively (on dried basis), were both kindly provided by The Navigator Company (Portugal).

2.2. DES preparation

The humidity of the individual components, [Ch]Cl and LA, was first measured with a Metrohm 831 Karl Fischer coulometer, being 10.4 and 6.8 wt%, respectively. Both [Ch]Cl and LA were weighed in a 1:10 molar ratio in sealed glass vials. The mixture was heated up to 70.0 °C and was kept at constant stirring until a transparent liquid was formed. The liquid was kept at this temperature for one hour before cooling down to room temperature, and was then kept in sealed glass vials at room temperature.

142

143 **2.3. Cellulose and xylan treatment with DES**

144 Samples of microcrystalline cellulose (MCC) or bleached kraft pulp (BKP) or xylan (0.150 g)
145 and [Ch]Cl:LA (3.0 g) were weighed into glass tubes. The tubes were sealed and placed in a
146 Radleys Carousel Tech and treatments were carried out at 130 ˚C for different periods of time (0.5,
147 1, 4, 8, 12, 16 and 24 h). After treatment, samples were cooled down to room temperature.
148 Subsequently, xylan and cellulose were precipitated with ethanol and water (200 mL),
149 respectively, stirred (800 rpm) overnight and recovered by vacuum filtration with Whatman®
150 nylon filters (0.45 μm porosity). The recovered solid samples were left on a ventilated oven at 40
151 ˚C overnight, while the liquid fractions were stored in a freezer.

152

153 **2.4. Wood treatment with DES**

154 Milled wood (300 mg) and [Ch]Cl:LA (3.0 g) were weighed into glass tubes. The tubes were
155 sealed and placed in a Radleys Carousel Tech and treatments were carried out at 130 ˚C for
156 different periods of time (1, 4 and 8 h). After treatments, tubes were cooled down to room
157 temperature. Then, 10 mL of a water:ethanol (1:1 w/w) mixture was added to reduce the viscosity
158 of the system and to maintain lignin soluble. The resulting mixtures were filtered by vacuum and
159 filtrates were recovered for lignin precipitation step. The solids were rinsed with water:ethanol
160 (1:1 w/w) mixture and placed in a ventilated oven at 40 ˚C overnight. Ice cold water was added to
161 the filtrate to precipitate lignin and the produced lignin fraction was filtered, recovered and placed
162 in the oven at the same conditions. The solid recovery yields were determined gravimetrically.
163 Two replicates were made for each condition.

164

2.5. Analytical characterization of solid and liquid fractions

Polysaccharides in their pristine form, the resulting solid and liquid fractions resulting from the treatments, as well as neat DES and DES after treatment, were characterized by different analytical techniques as described below.

2.5.1. Nuclear Magnetic Resonance (NMR)

Native xylans, as well as those obtained from DES or liquid fractions (~20 mg) were dissolved in deuterated dimethyl sulfoxide (DMSO-d6), with trimethyl silane (TMS) as internal reference, and the resulting solution was transferred into an NMR tube. ^{1}H NMR and ^{13}C NMR spectra were recorded using a Bruker Avance 300 equipment at 300.13 MHz and 75.47 MHz, respectively.

Cellulose samples were analyzed through ^{13}C solid-state cross-polarized magic-angle spinning nuclear magnetic resonance (^{13}C CP-MAS NMR). Spectra were recorded on a Bruker Avance 400 spectrometer. Samples (50 mg) were packed into a zirconia rotor sealed with Kel-F caps and spun at 7 kHz. Acquisition parameters were as follows: 4 μs 90° pulse width, 2 ms contact time, and 4 s dead time delay.

2.5.2. Fourier Transform Infrared with Attenuated Total Reflectance (FTIR-ATR)

The FTIR-ATR spectra of solid samples were acquired in a FTIR system Spectrum BX, PerkinElmer, equipped with a single horizontal Golden Gate ATR cell and a diamond crystal. Analyses were performed at room temperature with controlled air humidity. All data was recorded in the range of 4000-600 cm^{-1} by accumulating 32 scans with a resolution of 4 cm^{-1} and interval of 1 cm^{-1}. The acquired spectra were subtracted against background air spectrum and recorded as transmittance values.

FTIR-ATR was also used to estimate the degree of esterification (DE) of MCC and BKP samples after treatment with DES. Cellulose triacetate (DE=3), cellulose acetate (DE=2) and blended MCC with cellulose diacetate (DE=2) were used as standard samples to build a calibration curve recording the intensity of the vibrational band associated with the ester bond as function of DE (Figure S8 in Supporting Information (SI)). The calibration curve was validated with a confidence interval of 95% (Table S1 in SI).

2.5.3. X-Ray Diffraction (XRD)

X-ray diffraction patterns of cellulosic samples were determined using a Phillips X'pert MPD diffractometer using Cu Kα radiation. The XRD measurements were performed with a scan step size of 0.02° and a time *per* step of 2.5 s for a 2θ range between 4° and 40°. The crystallinity index (C.I.) of cellulosic samples were calculated as described elsewhere[37] using the following equation:

$$C.I = \frac{I_{200} - I_{am}}{I_{200}}, \quad (1)$$

where I_{200} is the maximum intensity (2θ of 22°–23°) at lattice peak (200) corresponding to crystalline fraction of cellulose, while I_{am} is the minimum intensity (2θ of 18°-19°) related to the amorphous part.

2.5.4. Scanning Electron Microscopy (SEM)

The surface morphology of MCC, BKP and *E. globulus* wood samples before and after 1, 4 and 8 h of [Ch]Cl:LA thermal treatment was analyzed by SEM. The samples were dried for 24 h in a

ventilated oven, covered with carbon and then analyzed using a Hitachi SU-70 microscope at 15kV.

2.5.5. Composition analysis of solid fractions

The chemical composition of the solid fractions obtained from wood treatments with [Ch]Cl:LA (1:10) was determined by following the National Renewable Energy Laboratory (NREL) standard protocol.[38] The solid samples were treated with sulfuric acid (72 wt%) at 30 °C for 1 h and were subsequently diluted with distilled water to a concentration of 4% sulfuric acid and autoclaved for 1 h at 121°C, enabling the polysaccharide acid hydrolysis. After this reaction, the samples were filtered to separate solid and liquid streams. The filtrate was analyzed by HPLC for the determination of sugar content (glucose and xylose), while the resulting solid was washed with 50 mL water and placed in an oven at 105°C for 24h. Finally, the solid samples were transferred to a furnace at 575 °C overnight. In the oven and furnace steps, insoluble lignin and ashes contents were determined gravimetrically.

2.5.6. High Performance Liquid Chromatography (HPLC)

. The liquid samples from xylan treatments with DES and from NREL acid hydrolysis protocol were injected in a HPLC Elite LaChrom, VWR Hitachi equipped with an autosampler – HITACHI L2200 and a Rezex ROA Organic Acids H^+ column (Phenomenex, USA). A Hitachi L-2490 refractive index detector (RID) and a Hitachi L-2455 diode array detector (DAD) were used for the analysis.

In case of xylan treatments, the obtained liquid fractions were diluted by taking into account the concentration of [Ch]Cl:LA. The samples were injected (10 µL) and analyzes were run at 65 °C

(oven Gecko 2000) for 80 min with a mobile phase composed of 0.01 N H_2SO_4 aqueous solution and a flowrate settled to 0.6 mL·min^{-1} using a Hitachi L-2130 pump. Glucose and xylose were detected by RID, while DAD (280 nm) was used in the detection of furfural.[39,40] Calibration curves for glucose, xylose and furfural standards were established. In xylan treatments, calculations on molar basis between consumed xylan and produced xylose and furfural were performed.

3. Results and Discussion

The research on biomass delignification with DES, and particularly with [Ch]Cl:LA (1:10), has shown promising results.[25,26,30] Although the obtained lignin fraction has been characterized as a highly pure and high-quality sample, the effect of [Ch]Cl:LA (1:10) on the chemical structure of cellulose was barely studied and the fate of hemicelluloses was practically disregarded. In this work, physicochemical and morphological modifications of model polysaccharides that may occur during thermal treatment with [Ch]Cl:LA (1:10) were investigated. Microcrystalline cellulose (MCC), bleached Kraft pulp (BKP) and xylans were chosen as model polysaccharide samples and their treatment with DES was performed at 130 ˚C for different time periods. After thermal treatment, solid samples were recovered and characterized by FTIR-ATR, NMR, SEM and XRD, while liquid samples were recovered and characterized by NMR and HPLC. The obtained results were compared to those of wood delignification assays mediated by [Ch]Cl:LA (1:10). The stability of the DES over time was also attempted.

3.1. Cellulose modification during DES treatment

The visual aspect and solid recovery yields of MCC and BKP change along the treatment with [Ch]Cl:LA (1:10) at 130 °C, as shown in Figure 1 and Table 1, respectively. BKP switched from a fluffy white to a brownish aspect, especially after 4 h of treatment onwards. This modification was slower in MCC samples, where a very light darkening of the recovered solid was observed only after 8 h. Nevertheless, the solid fractions of both samples reached a dark brown color after 24 h of treatment, demonstrating a negative effect of the treatment time. These results give a hint that some physicochemical and/or morphological modifications of cellulose occur in presence of [Ch]Cl:LA (1:10). Although at small extent, the formation of carbohydrate-derived chromophores (*e.g.* furanic compounds)[41,42] as consequence of acid-based degradation reactions of cellulose promoted by DES could be a cause for this fiber darkening.

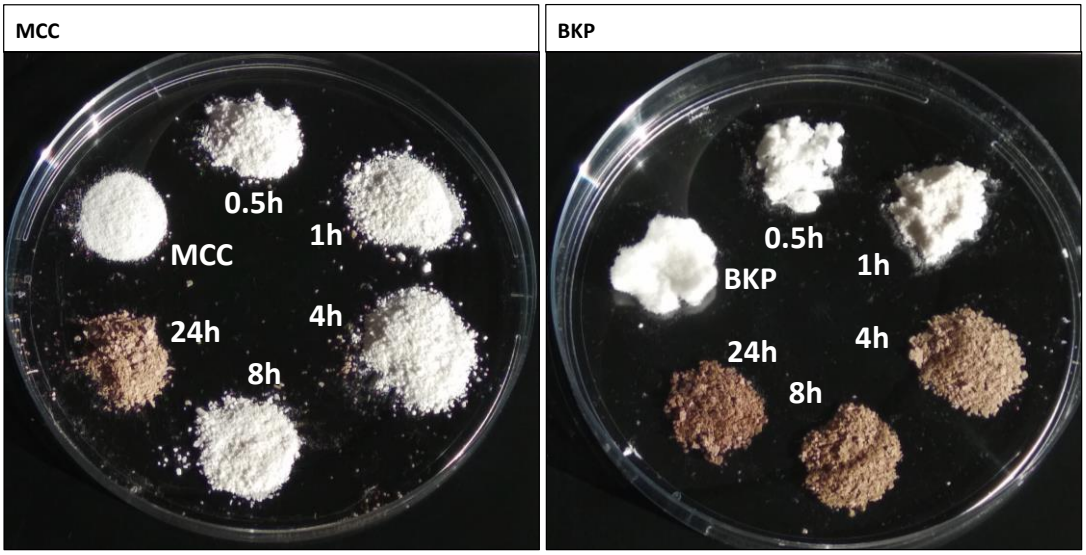

Figure 1. Visual aspect of MCC and BKP after settled periods of treatment with [Ch]Cl:LA (1:10) at 130 °C.

Regarding the solid recovery yield, there was no noticeable mass loss of MCC along the DES treatment, while for BKP treatments 92.9 wt% solid yield was obtained at 1h of treatment, following by an increase of yield that surpassed 100 wt%. The initial mass loss suggests a partial cellulose hydrolysis provided by the acidic medium, while the following mass increment can be associated with lactic acid esterification onto the fibers surface. These hypotheses will be further validated by the FTIR, NMR and SEM analyses discussed below.

Table 1. Solid recovery yields of MCC and BKP attained for different treatment times with [Ch]Cl:LA (1:10) at 130 °C.

Sample	Time [h]	Solid Yield [wt%]
MCC	1	96.5 ± 0.8
	4	99.3 ± 0.1
	8	99.7 ± 0.5
	24	100.8 ± 0.4
BKP	1	92.9 ± 0.6
	4	101.3 ± 0.6
	8	105.0 ± 1.1
	24	103.0 ± 1.2

More insights were given by FTIR-ATR analysis of cellulose samples before and after treatment with [Ch]Cl:LA (1:10). The FTIR spectra of MCC and BKP recovered solids are contrasted with those of the initial cellulose samples in Figure 2. In all cases, typical cellulose vibrational bands, at 3400 cm^{-1}, 2900 cm^{-1} and 1060 cm^{-1} were identified, being associated with O-H, C-H and C-O stretching vibrations, respectively (full spectra are presented in Figures S1 and S2 in SI). The bands at lower wavenumbers are related to the C-OH elongation vibrations (1200–1000 cm^{-1}) and

C-O-C stretching (1041–1035 cm^{-1}), which are also characteristic for cellulosic substrates.[43] These bands are observed in all spectra, meaning that the main chemical features of cellulose are kept after treatment with DES. However, an additional vibrational band at 1740 cm^{-1} appeared in treated cellulose samples and its intensity increased with the time of treatment. This band is attributed to unconjugated C=O bonds of ester groups that could be related to the esterification of cellulose hydroxyl groups with lactic acid.[44] Furthermore, the corresponding lactic acid C-H vibrational bands at 2850 cm^{-1} (Figures S1 and S2 in SI) and 1454 cm^{-1} are also noticeable. The degree of esterification (DE) with lactic acid was estimated for both MCC and BKP treated samples (Table S2) through validated quantitative analysis of the vibrational band at 1740 cm^{-1} (Tables S1 and Figure S8). Between 0.5 and 24 h of treatment, DE values in the ranges of 0.112-0.766 and 0.156-0.851 for MCC and BKP samples were found, respectively.

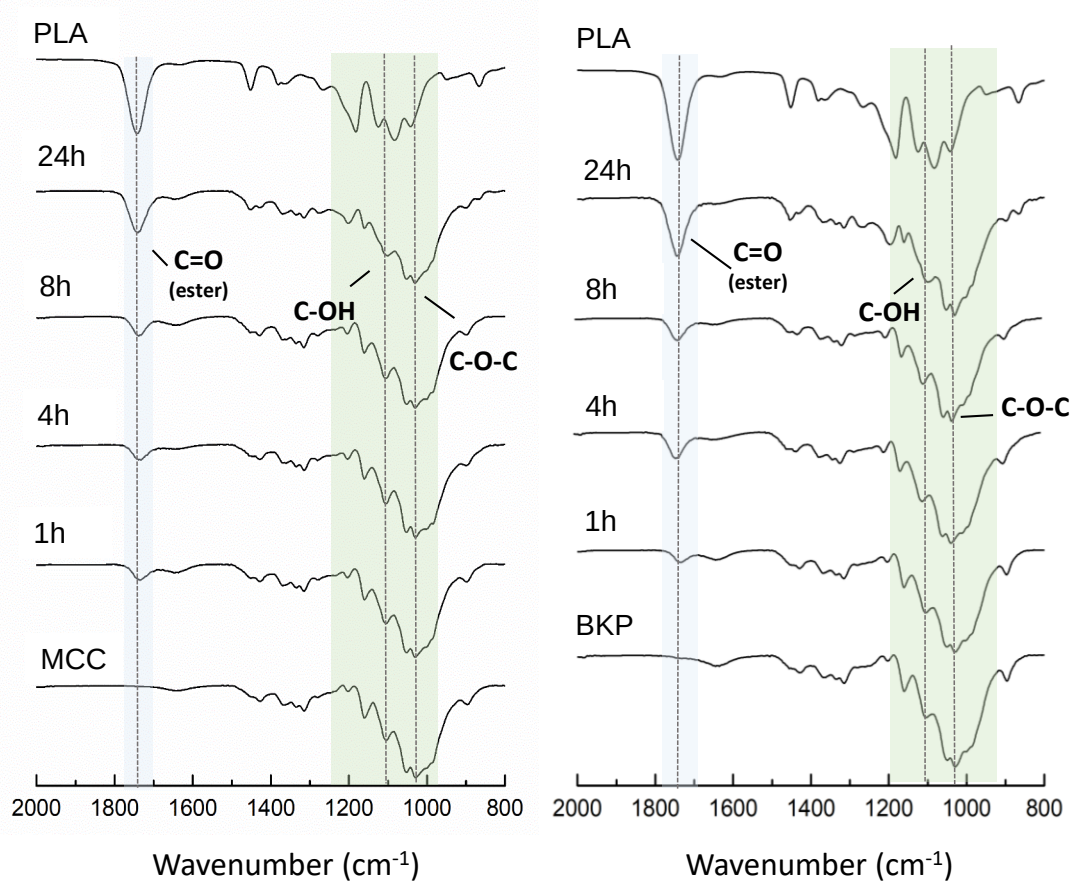

Figure 2. FTIR spectra of MCC (left) and BKP (right) after selected times of treatment with [Ch]Cl:LA (1:10) at 130 °C. The polylactic acid (PLA) spectrum is also shown as standard for the comparison of extra vibrational bands in cellulose samples.

The hypotheses of cellulose esterification with lactic acid was further supported by the ^{13}C solid-state NMR analysis of the MCC and BKP after DES treatment for 1, 4, 8 and 24 h (Figure S3 in SI). Both spectra of pristine MCC and BKP presented the typical cellulose resonances: C1 at 105.0 ppm, C4 at 86.4 ppm, C3 at 74.7 ppm, C2 and C5 in the region between 73.0 – 71.0 ppm, and the signal corresponding to C6 at 63.8 ppm.[45] On the other hand, the spectra corresponding to the recovered cellulose samples presented not only the typical cellulose resonances but also chemical shifts related to C=O (≈175 ppm) and CH_3 (≈20 ppm) groups assigned to lactic acid moieties. The

intensity of these extra signals increased with the treatment time as also observed in FTIR data, revealing a reaction between this organic acid and cellulose fibers by esterification. This kind of reaction was previously reported for functionalized cellulose nanocrystals with lactic acid.[46]

The recovered cellulose fractions were then analyzed by SEM to better address the microscopic morphological changes of the fibers after DES treatment. Figure 3 depicts the SEM images at different magnifications obtained for both MCC and BKP before and after treatment (1, 4 and 8 h) with [Ch]Cl:LA (1:10) at 130 °C. At 1h of treatment, no noticeable change was observed in MCC sample, while shorter BKP fibers were obtained in comparison to the native BKP. For both celluloses, agglomeration was observed (4 h), but BKP exhibited more extensive changes in its fiber morphology when compared with MCC. The fiber length reduced even further, while these short fibers agglomerated into a sheet-like structure similarly to that observed for MCC. On the contrary, after 4 and 8 h of treatment there is indeed agglomeration of MCC crystals, but their shape did not change substantially over time. These observations suggest that a substantial shortening in long BKP fibers is taking place during DES treatment, leading to a material with analogous morphology to that obtained with MCC treatment. This is in agreement with the mass loss discussed above suggesting partial hydrolysis of cellulose fibers in presence of DES, most likely the hydrolysis of cellulose amorphous regions.

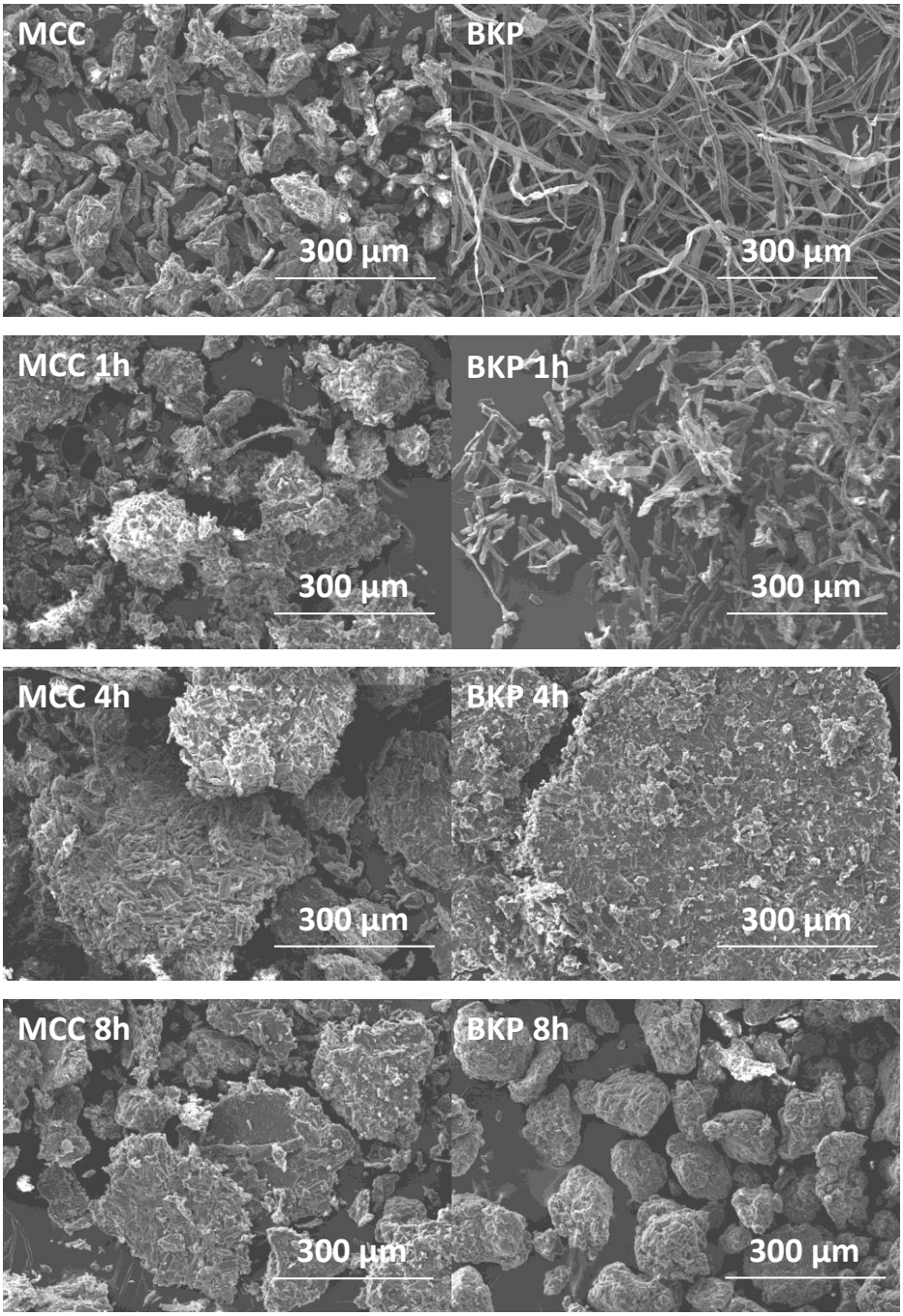

329

330 **Figure 3.** SEM images of MCC and BKP before and after settled periods of treatment with
331 [Ch]Cl:LA (1:10) at 130 °C. Microscopic magnification of x150.

332

333 The impact of DES treatment on cellulose crystallinity was evaluated by XRD analysis. The
334 crystallinity index values of each MCC and BKP solid samples are given in Table 2. The obtained

data reveal a decrease on cellulose crystallinity with the time of treatment. MCC crystallinity indexes decreased from 75.9 % to 73.6 %, while a higher decrease from 71.6 % to 66.3 % was observed for BKP samples. In literature, distinct results regarding the crystallinity of cellulose-rich solid fractions obtained after biomass processing with [Ch]Cl:LA (at similar conditions) were reported.[26,29] Kumar *et al.*[29] reached similar results showing a decrease of crystallinity between untreated wheat straw and the obtained cellulose-rich fraction. However, an opposite trend was reported by Shen *et al.*[26], who demonstrated an increase in the crystallinity after biomass treatment with [Ch]Cl:LA. The authors mentioned the removal of amorphous biomass components, such as lignin and xylan, as the major cause.[26] The slight decrease of cellulose crystallinity observed in the present work can be associated with the physicochemical modifications promoted by [Ch]Cl:LA (1:10) at 130 °C as discussed above.

Table 2. Crystallinity indexes of MCC and BKP after treatment with DES at 130 °C over time.

Sample	Time [h]	2θ range		Crystallinity index [%]
		I_{am}	I_{200}	
Native MCC	-	1227	5094	75.9
MCC	1	1657	6465	74.4
	4	1628	6466	74.8
	8	1354	5285	74.4
	24	1484	5621	73.6
Native BKP	-	3227	11358	71.6
BKP	1	1608	5916	72.8
	4	1978	6331	68.8
	8	2490	7498	66.8
	24	1746	5177	66.3

3.2. Xylans transformation with DES

Few studies have reported the extraction and valorization of xylans using DES as solvent media.[18,35,36] For instance, a xylan pre-extraction step from biomass was developed with the mild alkaline-based [Ch]Cl:Urea aiming at preserving the xylan structure.[35] On another perspective, the use of acid-based DES, such as [Ch]Cl:Oxalic acid and [Ch]Cl:Malic acid, allowed a favorable conversion of xylans into furfural.[18] Although some trends have been reported with acid-based DES, the fate of hemicelluloses during [Ch]Cl:LA delignification media has not been explored.

Aiming at better understanding the behavior of hemicelluloses under these delignification approaches, the thermal treatments of xylans in presence of [Ch]Cl:LA (1:10) performed in this work, disclose that this polysaccharide is much more labile than cellulose. After DES treatment, a major fraction of xylans was dissolved in the liquid phase, most likely due to its hydrolysis and conversion. In this sense, the liquid fractions were analyzed by HPLC for the quantification of xylose and furfural, identified as major formed compounds. The results obtained from xylans treatments with [Ch]Cl:LA (1:10) are illustrated in Figure 4.

These data clearly showed a progressive xylan conversion promoted by the acidic character of the DES. After the rapid conversion of xylans into xylose (it reaches a maximum of 80.1 mol% after 1 h), the last was converted into furfural that reached a maximum yield (23.1 mol%) after 24 h. The production of furfural was favored over time by the acidity of [Ch]Cl:LA (1:10). Nevertheless, this yield is far from those reported in the literature for [Ch]Cl-based DES comprising oxalic (55.5 mol%), malic (75.0 mol%) and glycolic (32.3 mol%) acids as HBDs.[18,36] Yet, furfural yield did not increase at the same rate as xylose consumption during time. This suggests that furfural may undergo degradation or polymerization,[47] leading to products which are not detected by HPLC (“others” in Figure 4) or are not water soluble (expressed in the solid

yield in Figure 4). This hypothesis was confirmed by looking at the sum of all identified components resulting from xylans conversion, which suffered a sharp decrease after 4 h. The amount of recovered solid obtained during the treatment is also intriguing, since a decrease of the recovered solid yield was obtained up to 4 h, while it increased after 8 h of treatment and onwards. This effect on the solid fraction was further studied by both FTIR-ATR and NMR (^{1}H and ^{13}C) techniques as discussed below.

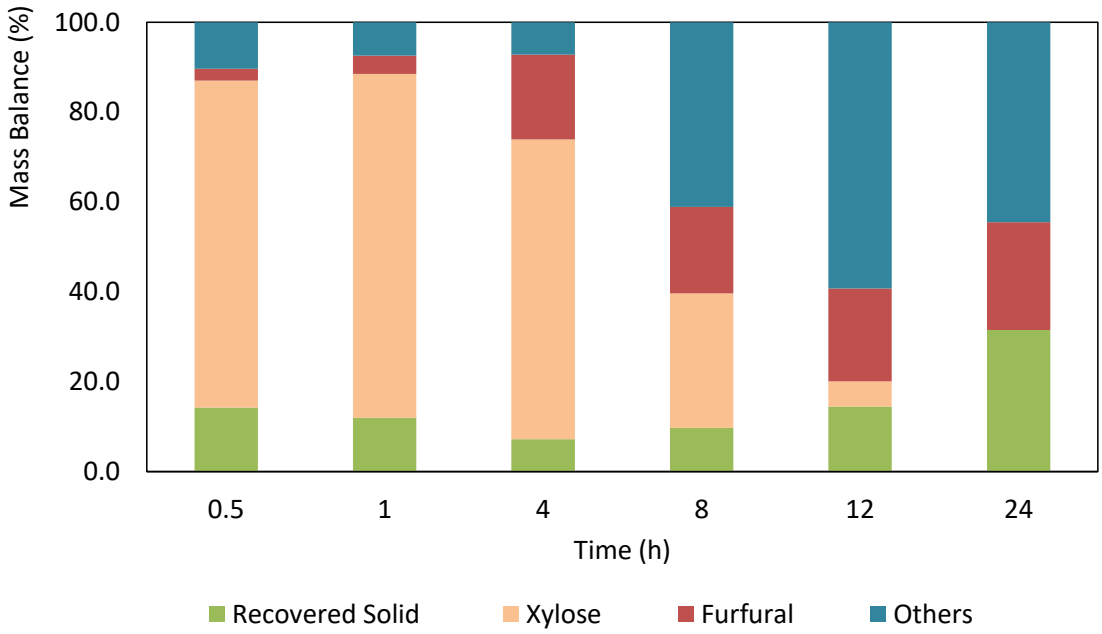

Figure 4. Xylans mass balance after DES treatment at 130 °C for different times expressed as the sum of recovered solid with both xylose and furfural yields (mol product/mol initial xylan) in the liquid phase. "Others" refers to products that were not detected in the DES liquid phase by the HPLC quantification method.

Figure 5 presents the FTIR spectra of pristine xylans and recovered solids after treatment with [Ch]Cl:LA (1:10) at different times (complete spectra can be found in Figure S4 in SI). The FTIR

spectra of pristine xylans present the typical vibrational bands of this polysaccharide class,[35,48] namely a band in the range 897 – 890 cm^{-1} associated with the β(1→4) glycosidic bond between the xylopyranose units of the xylan backbone, intense bands at 1200-1000 cm^{-1} corresponding to the C-OH elongation vibrations, and a maximum vibrational band at 1041-1035 cm^{-1} attributed to the C–O–C stretching of the pyranoid-ring of xylose. The bands observed between 1600 and 1500 cm^{-1} refer to xylan C-C bonds, while a xylan C-H bend absorbs at 1450-1400 cm^{-1}.

The acquired FTIR spectra showed that the chemical structure of the non-converted solid was mostly preserved during the first 4 h of treatment. Yet, a band at 1718 cm^{-1} (attributed to unconjugated C=O bonds of lactic acid carboxylic group) appeared after only 30 min. Like in the case of cellulose, a possible esterification of xylan with lactic acid may occur in the presence of [Ch]Cl:LA. This band was detected in all spectra of recovered solids (in those at 4 and 8 h of treatment, the water bending vibration, 1650 cm^{-1},[49] masked the carbonyl band, as consequence of moisture absorption).

For treatments longer than 4 h, the absence of the bands related to the xylan backbone was verified, and different bands at 1192, 1123, 1088 and 1041 cm^{-1} appeared instead. These vibrational bands can be found in the lactic acid spectrum (see Figure 12, as further discussed), but also in the polylactic acid FTIR spectrum (Figure 5). However, the intensities of those bands are characteristically different between lactic acid and polylactic acid, making the FTIR spectrum a fingerprint of each analyte. By comparison, the specific pattern of these vibrational bands observed in the FTIR spectrum of the solid obtained after 12 and 24 h of treatment was analogous to that of polylactic acid. A similar pattern was also detected in the FTIR spectrum of xylan-lactide copolymer reported by Zhang *et al.*[50] This means that grafting of lactic acid oligomers from xylans or homopolymerization of lactic acid was enabled for prolonged times of treatment.

410

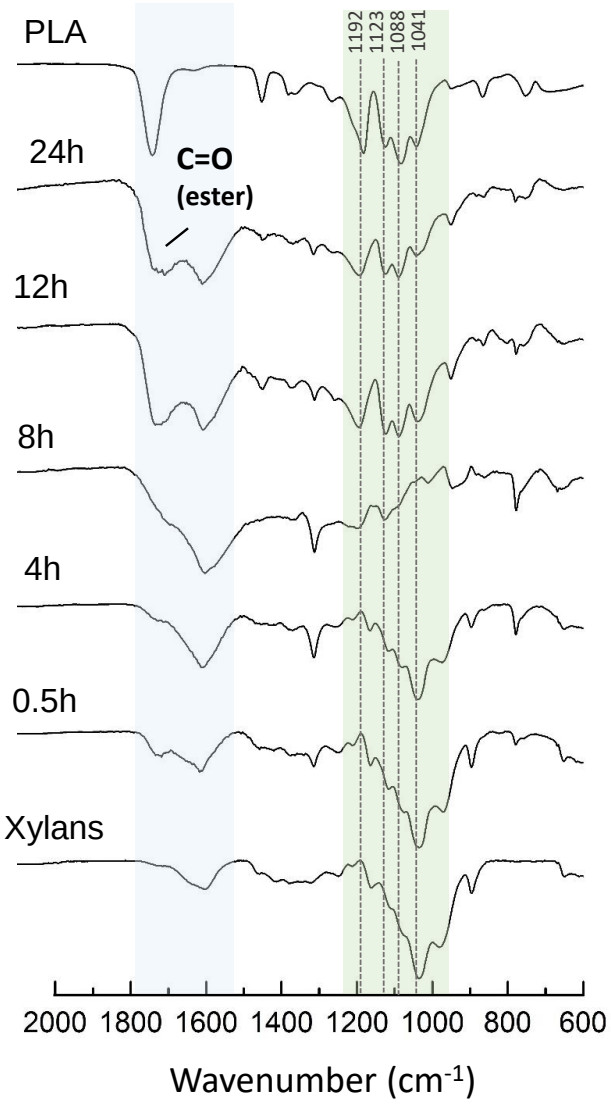

411

412 **Figure 5.** FTIR spectra of pristine xylans and recovered solids obtained after treatment with
413 [Ch]Cl:LA (1:10) at 130 °C at different times. The PLA spectrum is also shown as standard for
414 the comparison of extra vibrational bands.

415

416 In Figure 6 the ^{1}H NMR spectra of pristine xylans and the recovered solids after treatment with
417 [Ch]Cl:LA (1:10) at different periods are given. The structure of pristine xylan with corresponding

418 chemical shift assignments is also depicted. Overall, the pristine xylan ^{1}H NMR presented the
419 typical resonances from all the different protons of the non-substituted β-D-xylopyranose ((1→4)-
420 β-D-Xylp) residues between δ 4.36 and δ 2.62 ppm.

421 Although the xylan backbone signals were preserved in the ^{1}H NMR spectrum of residual xylan
422 after 4 h of treatment (supported by FTIR-ATR results), new proton signals appeared between 1.00
423 and 1.60 ppm. All these signals are expected to be associated with CH_3 groups of lactic acid in
424 different chemical environments, *i.e.*, in lactic acid isomers, lactide isomers and polymerized lactic
425 acid (discussed in more detail below). Zhang *et al.*[50] provided a study on the synthesis of a
426 thermoplastic derivative of xylan prepared by grafting polymerization of lactide from xylan
427 backbone, where the same signals appeared in the ^{1}H NMR spectrum and were attributed to
428 chemical shifts of protons in CH_3 groups of lactic acid grafting from xylan.[50] On the other hand,
429 after 16 h of treatment, the signals from xylan backbone practically disappeared (Figure 6). Instead,
430 only a single broad signal appears at 3.06 ppm (unassigned) related to CH_3 or CH_2 alike chemical
431 shifts as well as the signals assigned to CH_3 groups of lactic acid moieties.

432 Overall, the recovered solid is mostly composed of non-hydrolyzed xylan for short periods of
433 treatment, while at longer periods the solid yield increases as consequence of water insoluble by-
434 products (dark precipitate) formed by side reactions. It includes lactic acid grafting from xylan or
435 lactic acid homopolymerization, as observed by FTIR-ATR analysis, or degradation of xylose and
436 furfural into polymeric structures often called humins.[51,52]

437

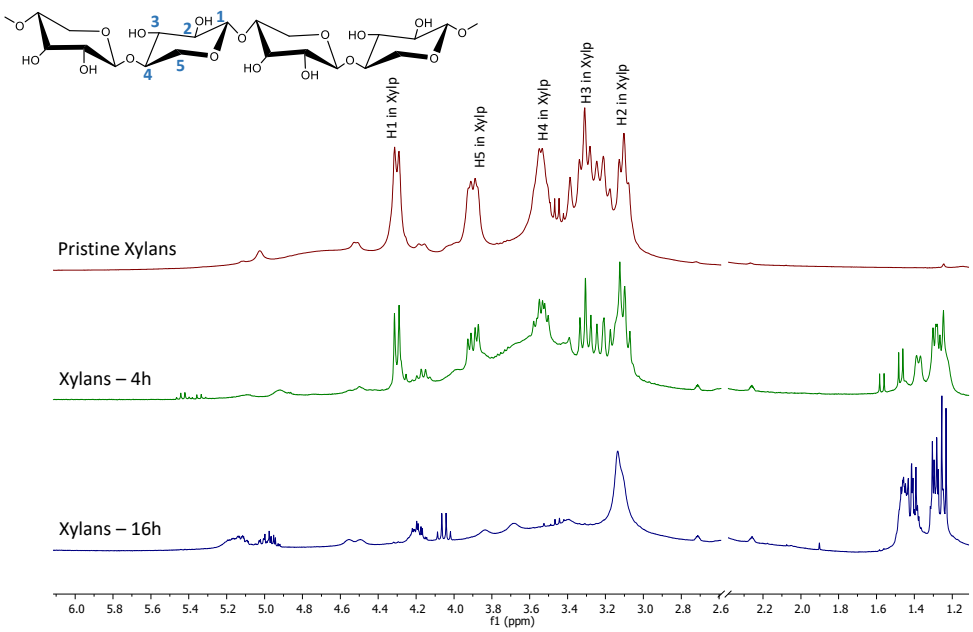

Figure 6. ^{1}H NMR spectra of pristine xylans and recovered solids after 4 and 16 h of treatment at 130 °C with DES. Solvent peak was cut out from each spectrum for a clear presentation.

3.3. Wood treatment with DES

The results disclosed in the last two sections give a perspective of possible reactions and morphological changes in polysaccharides that might take place during biomass delignification process using [Ch]Cl:LA (1:10). Yet, the biomass recalcitrance, which means chemical linkages between polysaccharides and lignin, the presence of lignin itself and other biomass components could directly influence the degree of those modifications. Therefore, data acquired from MCC, BKP and xylans treatments was contrasted with thermal treatments of real wood samples.

Milled *E. globulus* wood was treated with [Ch]Cl:LA (1:10) at 130 °C for 1, 4 and 8 h. After treatments, recovered solids enriched with cellulose fibers were morphologically and chemically characterized, while the liquid fractions were analyzed for the determination of xylose and furfural contents analogous to xylans assays. In addition, a lignin-rich fraction was isolated from the DES

liquid phase after treatment and its recovery yield was also calculated. Figure 7 compiles the data of these wood treatments.

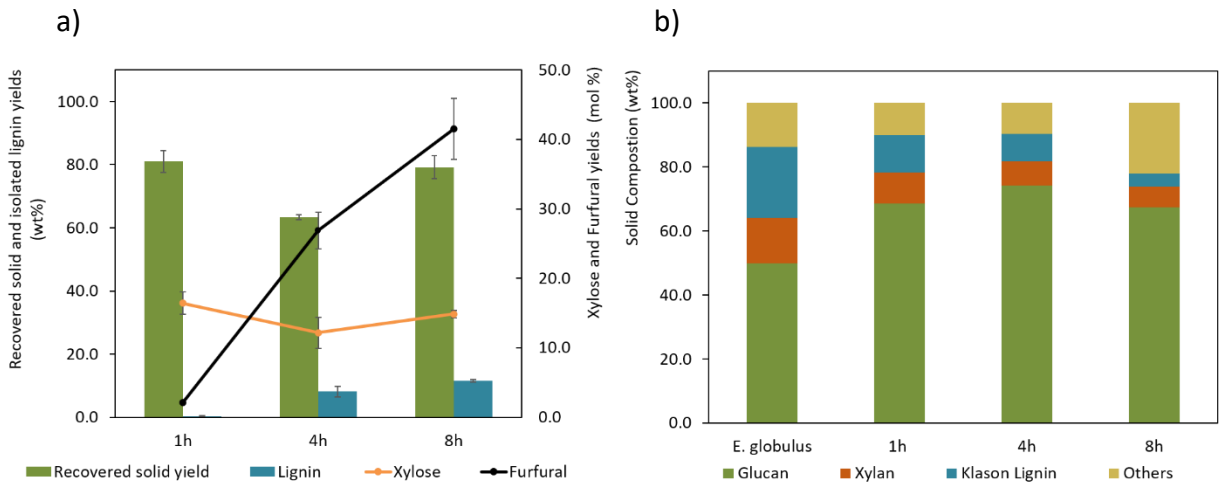

Figure 7. a) recovered solid and isolated lignin yields ($wt_{sample}/wt_{initial\ wood}$) plotted with xylose and furfural yields ($mol_{product}/mol_{initial\ xylan}$) during the *E. globulus* wood treatment (S/L=0.1) with [Ch]Cl:LA (1:10) at 130 °C at different times (1, 4 and 8 h). b) chemical composition of *E. globulus* wood and recovered solids.

The results obtained show that the recovered solid yield decreases from 1 to 4 h of treatment to a minimum of 63.3 wt%, while it considerably increased up to 8 h.

The visual aspect of the solids (Figure 8) demonstrated that similarly to the results obtained for MCC and BKP treatments, those produced after 1 and 4 h of treatment presented a light color. The first is still comparable to the initial milled wood morphology, while a pulp-like solid was observed for the second condition, suggesting an effective delignification with [Ch]Cl:LA (1:10) at 4 h. This is further evidenced by the chemical composition of the recovered solid obtained at 4 h of treatment. The lignin content reduced substantially (from 20.5 wt% in initial wood to 8.4 wt.%), while simultaneous increase of the glucan content (from 50.0 wt% in initial wood to 74.1 wt.%)

was observed (Figure 7b). Moreover, the negligible yield of isolated lignin obtained at 1 h and further recovery of 8.1 wt% at 4 h (Figure 7a) also confirms the delignification. Although comparable pulp-like morphology was found for the solid at longer treatment (8 h), its dark brown aspect indicates degradation. Equivalent to model polysaccharides treatments, the formation of carbohydrate-derived chromophores and humins, as well as lactic acid esterification and grafting onto cellulose fibers and xylans may explain the high solid recovery yield at prolonged treatments. This is representative of the increased content of "others" from 9.7 wt% to 22.1 wt% and simultaneous decrease of glucan content from 74.1 wt% to 67.4 wt%, when contrasting the chemical composition of the recovered solids at 4 h and 8 h of treatment, correspondingly. These results are in line with the trend of the solid yield observed in BKP treatments.

Figure 7 also reveals the formation of xylose and furfural during wood treatment with DES. The amount of xylose in the liquid phase was practically maintained between a range of 10-20 mol% from 1 to 8 h of treatment, while a crescent production of furfural up to 41.5 mol% was observed in the same period. The presence of both xylose and furfural in the liquid fraction throughout the wood treatment correlates with the decrease of xylan content in the recovered solids, which reaches a minimum of 6.3 wt.% at 8 h. In all experiments, the xylose yields were much lower than those obtained in assays conducted with pristine xylans (Figure 4). On the contrary, the furfural yields at 4 and 8 h were higher in these wood treatments. The observed differences in xylose and furfural yields between pristine xylans and wood assays could be associated with the initial xylans/DES ratio. Xylans/DES ratios of 0.045 and 0.013 (dry basis) were used in experiments using pristine xylans and wood, respectively, that influences the kinetics of xylose production (hydrolysis) and furfural formation (dehydration). Furthermore, the intricate wood matrix and the presence of other

components in wood, such as cellulose and lignin, might also affect the production and stability of xylose and furfural in the DES medium.

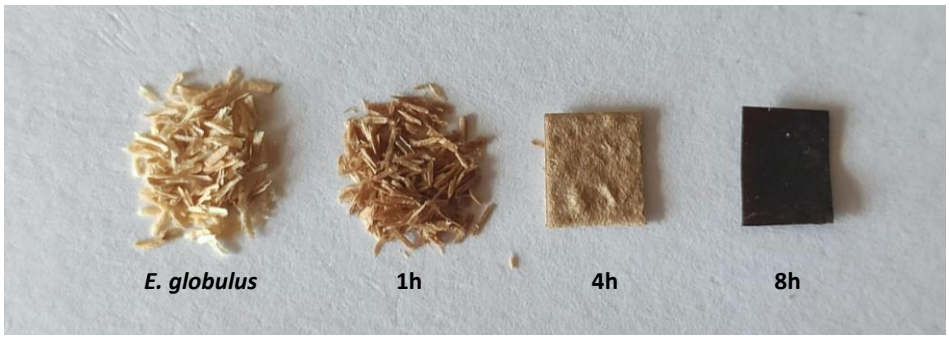

Figure 8. Visual aspect of recovered solids after thermal treatment of *E. globulus* wood with [Ch]Cl:LA (1:10) for 1, 4 and 8 h.

The recovered solids enriched with cellulose fibers were then analyzed by FTIR-ATR (the acquired spectra are displayed in Figure S5). The data demonstrated the delignification efficiency of [Ch]Cl:LA (1:10). For instance, typical lignin vibrational bands associated with the aromatic skeletal vibration (*e.g.* 1512 and 1600 cm^{-1}) were absent in the spectra of recovered solids obtained at 4 and 8 h of treatment. However, all spectra also demonstrated an intensity increase of the band at 1740 cm^{-1}, attributed to the esterification with lactic acid. This is a deviation from the natural occurring band at 1731 cm^{-1} in *E. globulus* wood FTIR spectrum referred to C=O stretching of ester groups in both lignin and hemicelluloses structures[53,54]. These results are in agreement with those obtained with MCC, BKP and xylans treatments, revealing that [Ch]Cl:LA (1:10) reacts with biomass during delignification processes allowing lactic acid esterification with cellulose fibers as well as grafting from xylan backbone.

The solid state ^{13}C NMR of recovered solids also confirmed the delignification performance of [Ch]Cl:LA (1:10) (Figure 9). At 1 h of treatment, the NMR spectrum depicted lignin characteristic

chemical shifts, including an intense signal at 56.7 ppm related to the carbons in lignin methoxy groups (O-CH_3), and low but broad intensities at 130-160 ppm associated with lignin aromatic carbons (C_{AR}-O and C_{AR}-C). This result indicates that 1 h of treatment is not enough for an efficient delignification. As the treatment goes onwards (4 and 8 h), these lignin signals disappeared, while those assigned to lactic acid increased, namely at ≈15 ppm (CH_3) and ≈175 ppm (C=O), corroborating the chemical modifications discussed above with FTIR data.

10.1002/cssc.202002301

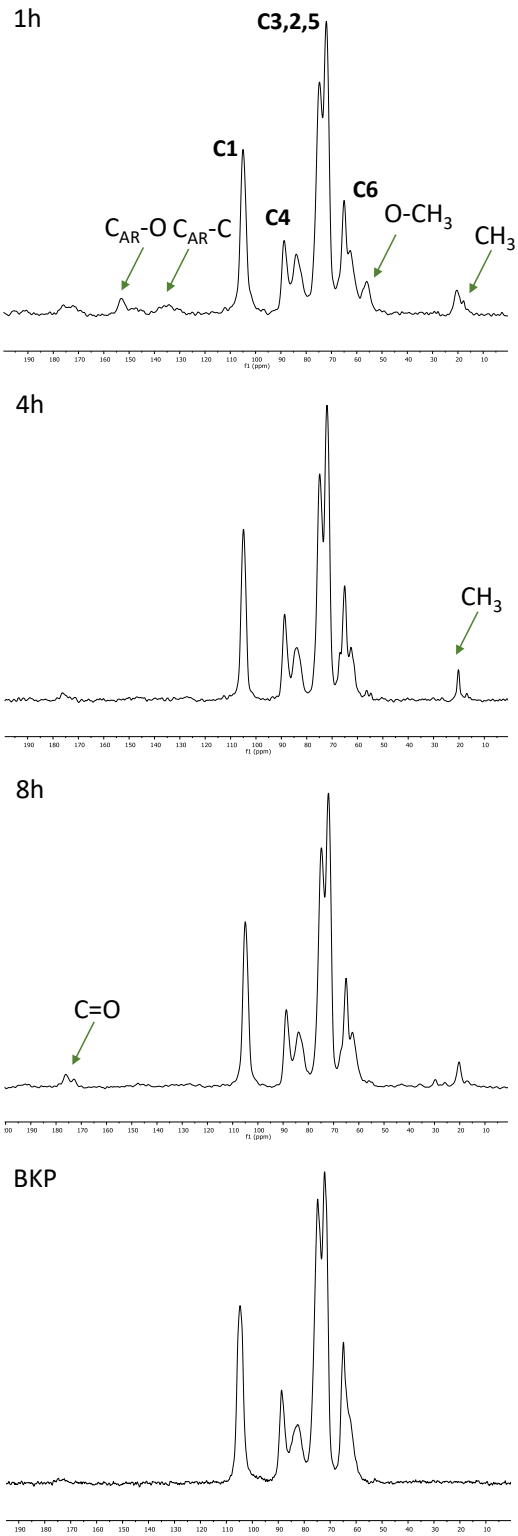

518

519 **Figure 9.** Solid state CP-MAS ^{13}C NMR of recovered solid samples after *E. globulus* wood

520 treatment (1, 4 and 8 h) with [Ch]Cl:LA (1:10) and BKP as standard cellulose sample.

521

522 The microscopic morphology of the resulting cellulose fibers was also evaluated by SEM
523 technique. Figure 10 shows the SEM images at different magnifications of native *E. globulus* wood
524 and recovered solids from thermal treatments with [Ch]Cl:LA (1:10). At microscopic
525 magnifications of x150 and x500 (first and second column), the strong organization of cellulose
526 fibers in native wood was observed, while the recovered solids exhibited disorganized fibers as
527 consequence of the matrix disruption mediated by DES action. The images clearly evidence the
528 presence of cellulose fibers, as expected by taking into consideration the delignification ability of
529 this DES,[25,55] and is corroborated by the spectroscopic analyses shown before. However, the
530 reaction media showed a considerable impact on fibers morphology. The obtained fibers partially
531 preserved their shape after 4 h, while they were considerably damaged after 8 h, analogous to BKP
532 treatments. At the longest treatment, the obtained fibers showed surface functionalization with
533 lactic acid as described before, including esterification of cellulose fibers, grafting of lactic acid
534 oligomers from xylan backbone as well as homopolymerization of lactic acid.

535

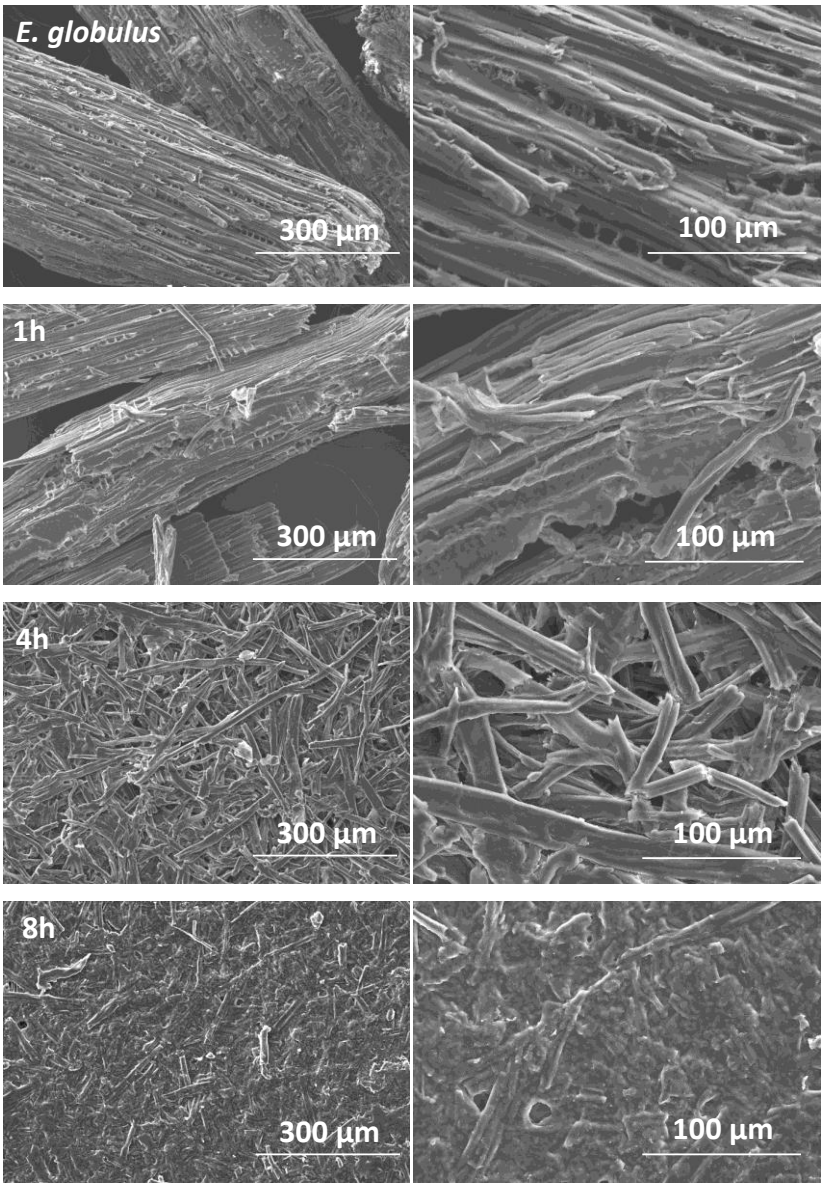

536

537 **Figure 10.** SEM images of native *E. globulus* wood and recovered solids from thermal
538 treatments with [Ch]Cl:LA (1:10) at 130 °C for 1, 4 and 8 h. Microscopy magnifications of x150
539 (left column) and x500 (right column).

540

541 Briefly, cellulose or biomass treatment with [Ch]Cl:LA (1:10) induces substantial damage on
542 cellulose fiber length, especially at prolonged treatments. Despite this impact in morphology, there
543 is limited weight loss and cellulose molecular features are preserved as shown by NMR, FTIR and

XRD data. For increased treatment time, lactic acid esterification onto cellulose surface was observed, which accounts for some increment in fiber recovery yield and most certainly to the agglomeration of fibers observed by SEM. Therefore, short residence time is recommended to avoid extensive modification of cellulose fibers preserving their physicochemical properties as much as possible. On the other hand, targeting functional cellulose-based materials with lactic acid (or other organic counterparts) could be an interesting approach[56] by using DES treatment with longer residence times. Nevertheless, data regarding the mechanical properties of those cellulose fibers are required to ascertain a successful application. On the other hand, xylans are easily converted allowing for xylose and furfural co-production. The reaction kinetics of those compounds however changes dramatically when dealing with the conversion of standard xylan or xylan incorporated in wood matrix. Nevertheless, it is clear that prolonged times leads to furfural degradation and formation of hemicellulose-derived insoluble products that affects the quality of the cellulose fibers as shown by the obtained solid at 8 h of treatment in Figure 8.

3.4. DES stability

Although [Ch]Cl:LA (1:10) is an outstanding DES for biomass delignification, this solvent should be properly exploited aiming to minimize its degradation. The stability of [Ch]Cl:LA (1:10) during thermal treatment was evaluated by NMR and FTIR-ATR. Figure 11 presents the ^{13}C NMR spectra and chemical shift assignments of [Ch]Cl:LA (1:10) before and after being subjected to thermal treatment at 130 °C during 8 h. The freshly prepared DES presented the typical resonances related to LA, namely at 178.32, 76.23 and 20.51 ppm assigned to carbons from COOH, C-OH and CH_3 groups, respectively. Less intense signals associated with [Ch]Cl carbons, such as C-OH at 68.1 ppm and the corresponding CH_2 and CH_3 groups at 56.11 and 54.65 ppm were also

depicted. Although DES was freshly prepared from pure grade reagents, the spectrum of neat DES presented other signals not related to either LA or [Ch]Cl. These chemical shifts were assigned to lactide, a by-product formed by condensation of two molecules of lactic acid,[57] becoming more pronounced after thermal treatment. Moreover, a severe decrease of the integrals of lactic acid carbon resonances was observed after thermal treatment, while other resonances related to carbons from lactic acid derivatives (including lactide) appeared (Figure 11). In fact, the 1:10 proportion between [Ch]Cl and LA, which is easily visible in the spectrum of fresh DES, seems to disappear after the applied thermal treatment. The lactide formation can also corroborate the polymerization of lactic acid since it is a common intermediate in this process. The DES degradation and side product formation can also be observed in the ^{1}H NMR spectra (Figure S6 in SI).

To further investigate the DES stability, [Ch]Cl:LA was analyzed by FTIR-ATR before and after the thermal treatment. Figure 12 presents the FTIR spectra of [Ch]Cl, LA and PLA (DP=500) as standard samples for the comparison with the FTIR spectra of DES before and after thermal treatment. Since an excess ratio of LA to [Ch]Cl exists, the DES spectrum is very similar to that of LA. Both LA and [Ch]Cl:LA (1:10) spectra presented the typical vibrational bands of lactic acid as described elsewhere,[58] including the C=O stretching band at 1720 cm^{-1} characteristic of carboxylic acid group, the region between 3000 and 2500 cm^{-1} representing the O–H stretching of the acid (full spectra can be found in Figure S7 in SI), and region below 1200 cm^{-1} that represents different kinds of C-H, C-O, and CH_3 vibrations (rocking, deformation, stretching).[58]

10.1002/cssc.202002301

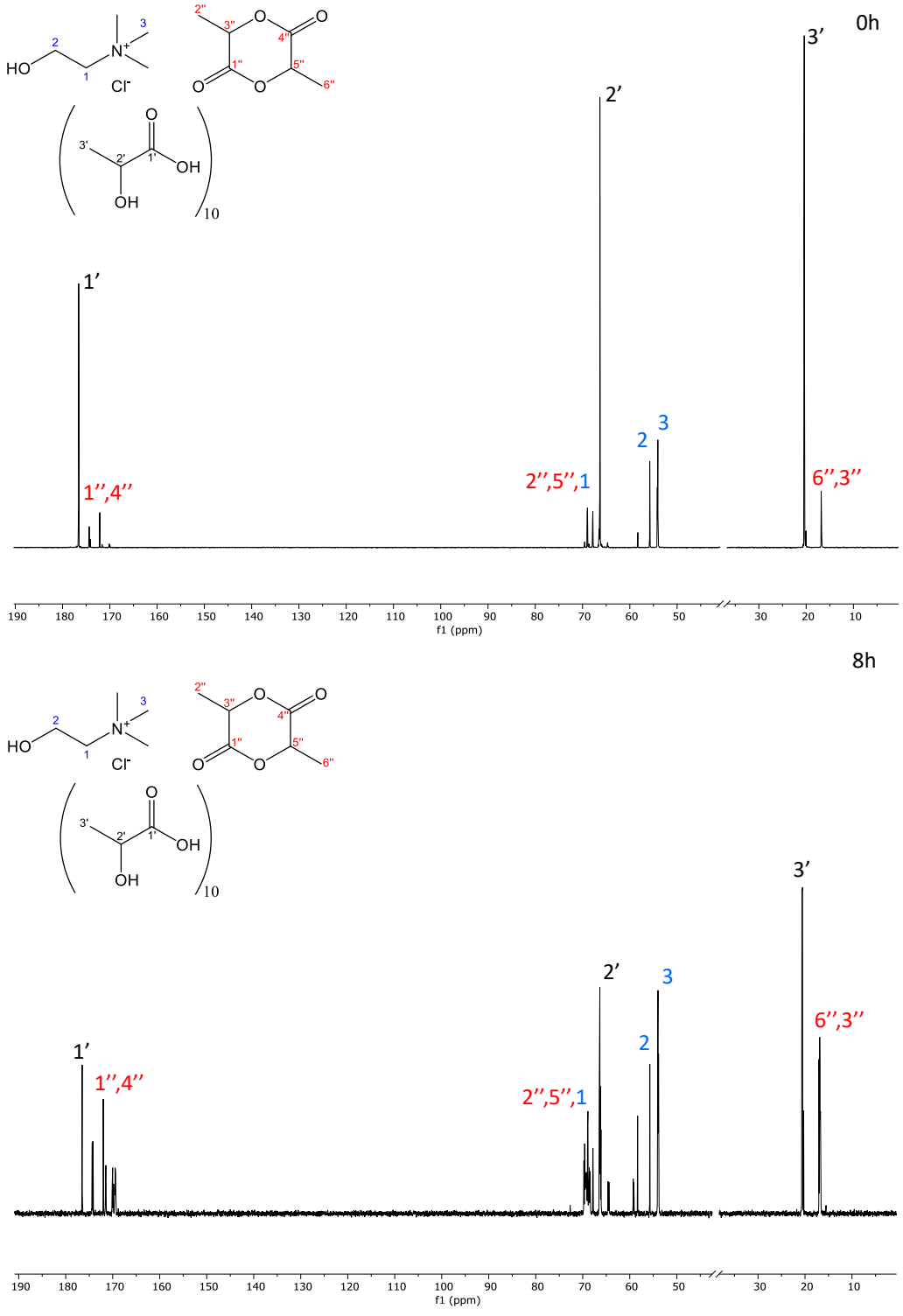

Figure 11. ^{13}C NMR spectra of [Ch]Cl:LA (1:10) before (top) and after thermal treatment at 130 ˚C for 8 h (bottom). Solvent peak was cut out from each spectrum for a clear presentation.

After thermal treatment, the FTIR spectrum of DES changed considerably, sharing common bands with the PLA spectrum. An example is a pronounced band at 1740 cm^{-1}, assigned to the C=O bond vibration, which is a clear shift of this signal from that of the neat DES spectrum (1720 cm^{-1}). Besides, others bands were commonly present in both treated DES and PLA standard spectra, including those attributed to C-O and C-O-C stretching vibrations (1182, 1129 and 1086 cm^{-1}) and C-CH_3 bond (1045 cm^{-1}).[44,59] Once more, there is a clear shift between the bands displayed in the spectrum of fresh DES when compared to that of treated DES, demonstrating that chemical modifications occur during the thermal process. These modifications seem to consist mainly in the lactic acid esterification when subjected to 130 ˚C, resulting in the polymerization of lactic acid. This phenomenon is further supported by the decrease of the integrals of lactic acid carbon signals displayed in the ^{13}C NMR spectrum (Figure 11), as well as by the appearance of same FTIR bands observed in the recovered xylan (Figure 5). Thus, it is likely that lactic acid self-reacts (homopolymerization) and it may also react with the polysaccharide hydroxyl groups by esterification and grafting. A similar grafting phenomenon was reported in a recent study showing the esterification of lactic acid oligomers with an hydroxyl group of a lignin model compound in the presence of [Ch]Cl:LA (1:10).[34] Overall, these results suggest that not all DES are stable and that caution should be considered when using these solvents at harsh conditions, such as high temperatures and acidic media.

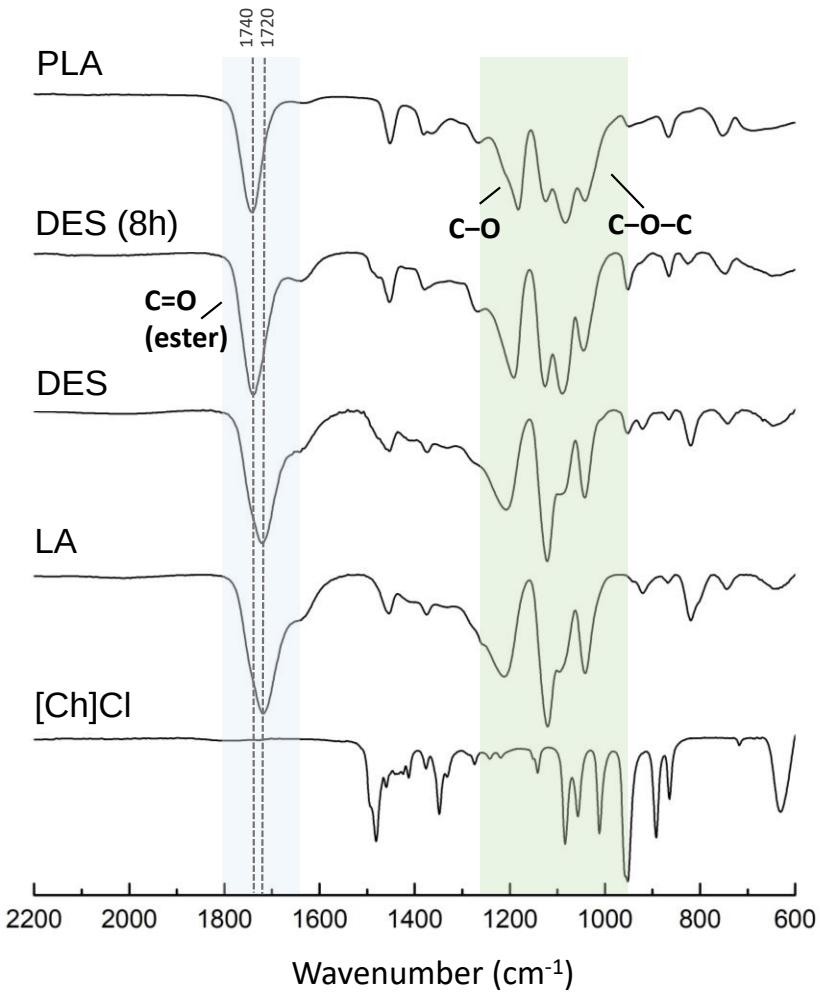

609

610 **Figure 12.** FTIR spectra of [Ch]Cl, lactic acid, [Ch]Cl:LA (1:10) before and after thermal
611 treatment (8 hours at 130 ˚C), and PLA (M_w=500).

612

613 **4. Conclusions**

614 The present work demonstrated a variety of physicochemical and morphological modifications
615 that polysaccharides undergo during thermal treatment with [Ch]Cl:LA (1:10). The treatment of
616 both microcrystalline cellulose and bleached kraft pulp using this DES at 130 °C unveiled the
617 occurrence of esterification between cellulose fibers and lactic acid over time, fiber shortening and
618 agglomeration. The darkening of cellulose fibers could be related to the formation of carbohydrate-

derived chromophores and humins. On the other hand, xylans are susceptible to extended hydrolysis mediated by DES producing xylose, while the formation of furfural and side reactions (lactic acid grafting and homopolymerization) were further observed at prolonged times of treatment. In wood processing, the occurrence of all these reactions was confirmed, which directly impact the quality of produced cellulose fibers as well as the valorization of the hemicellulose fraction. Furthermore, the degradation of DES during time was verified, changing the composition of the solvent. Lactic acid derivatives (*e.g.* lactide) and lactic acid polymerization were identified through NMR and FTIR-ATR analyzes.

Although [Ch]Cl:LA (1:10) has demonstrated high efficiency to extract a high-quality lignin fraction from biomass, the careful handling of this solvent must be performed. The identified drawbacks could be circumvented by applying treatments with short periods of time to minimize modification of cellulose fibers and unwanted side reactions of other biomass components and of the solvent as well. Optimizing the use of [Ch]Cl:LA (1:10) for short treatment periods would enable a sustainable biomass fractionation into good quality cellulose fibers, isolated lignin, xylose/furfural co-production along with solvent recyclability. Nonetheless, targeting functional cellulose-based materials grafted with organic acids, like lactic acid, could be an opportunity and alternative pathway for cellulose upgrading, rather than a pulp and paper valorization framework. This can be achieved using [Ch]Cl:LA (1:10) for long treatment periods.

Acknowledgments

This work was developed within the scope of the project CICECO-Aveiro Institute of Materials, UIDB/50011/2020 & UIDP/50011/2020, financed by national funds through the FCT/MCTES. The authors would like to thank the members of the ISPT “Deep Eutectic Solvents in the pulp and

paper industry" consortium for their financial and in-kind contribution. This cluster consists of the following organizations: Altri – Celbi, Buckman, Crown Van Gelder, CTP, DS Smith Paper, ESKA, Essity, Holmen, ISPT, Mayr-Melnhof Eerbeek, Metsä Fiber, Mid Sweden University, Mondi, Omya, The Navigator Company, Sappi, Essity, Smurfit Kappa, Stora Enso, Eindhoven University of Technology, University of Aveiro, University of Twente, UPM, Valmet Technologies Oy, Voith Paper, VTT Technical Research Centre of Finland Ltd, WEPA and Zellstoff Pöls. Furthermore, this project received funding from the Bio-Based Industries Joint Undertaking under the European Union's Horizon 2020 research and innovation programme under grant agreement Provides No. 668970 and was co-funded by TKI E&I with the supplementary grant 'TKI-Toeslag' for Topconsortia for Knowledge and Innovation (TKI's) of the Ministry of Economic Affairs and Climate Policy. The work was also funded by FCT/MCTES through the projects DeepBiorefinery (PTDC/AGR-TEC/1191/2014) and MultiBiorefinery (POCI-01-0145-FEDER-016403). The NMR spectrometers are part of the National NMR Network (PTNMR) and are partially supported by Infrastructure Project Nº 022161 (co-financed by FEDER through COMPETE 2020, POCI and PORL and FCT through PIDDAC). E. S. Morais acknowledges FCT/MCTES for a PhD grant (SFRH/BD/129341/2017). A. M. da Costa Lopes acknowledges ISPT for funding his postdoctoral grant.

References

[1] R. A. Sheldon, *J. Mol. Catal. A Chem.* **2016**, *422*, 3–12.

[2] N. Dahmen, I. Lewandowski, S. Zibek, A. Weidtmann, *GCB Bioenergy* **2019**, *11*, 107–117.

[3] G. De Bhowmick, A. K. Sarmah, R. Sen, *Bioresour. Technol.* **2018**, *247*, 1144–1154.

[4] F. Cherubini, *Energy Convers. Manag.* **2010**, *51*, 1412–1421.

[5] M. H. L. Silveira, A. R. C. Morais, A. M. Da Costa Lopes, D. N. Olekszyszen, R. Bogel-Łukasik, J. Andreaus, L. Pereira Ramos, *ChemSusChem* **2015**, *8*, 3366–3390.

[6] H. Zabed, J. N. Sahu, A. N. Boyce, G. Faruq, *Renew. Sustain. Energy Rev.* **2016**, *66*, 751–774.

[7] A. M. Da Costa Lopes, R. Bogel-Lukasik, *ChemSusChem* **2015**, *8*, 947–965.

[8] S. Gillet, M. Aguedo, L. Petitjean, A. R. C. Morais, A. M. Da Costa Lopes, R. M. Łukasik, P. T. Anastas, *Green Chem.* **2017**, *19*, 4200–4233.

[9] X. Zhao, L. Zhang, D. Liu, *Biofuels, Bioprod. Biorefining* **2012**, *6*, 561–579.

[10] M. I. Voronova, O. V. Surov, S. S. Guseinov, V. P. Barannikov, A. G. Zakharov, *Carbohydr. Polym.* **2015**, *130*, 440–447.

[11] M. C. Li, Q. Wu, K. Song, S. Lee, Y. Qing, Y. Wu, *ACS Sustain. Chem. Eng.* **2015**, *3*, 821–832.

[12] A. W. Carpenter, C. F. De Lannoy, M. R. Wiesner, *Environ. Sci. Technol.* **2015**, *49*, 5277–5287.

[13] C. Vilela, C.; Pinto, R.; Pinto, S.; Marques, P.; Silvestre, A.; Freire, *Polysaccharide Based Hybrid Materials Metals and Metal Oxides, Graphene and Carbon Nanotubes*, Springer, **2014**.

[14] H. Amiri, K. Karimi, *Bioresour. Technol.* **2018**, *270*, 702–721.

[15] A. Mukherjee, M. J. Dumont, V. Raghavan, *Biomass and Bioenergy* **2015**, *72*, 143–183.

[16] M. Yadav, D. K. Mishra, J. S. Hwang, *Appl. Catal. A Gen.* **2012**, *425–426*, 110–116.

[17] W. Wang, J. Ren, H. Li, A. Deng, R. Sun, *Bioresour. Technol.* **2015**, *183*, 188–194.

[18] E. S. Morais, M. G. Freire, C. S. R. Freire, J. A. P. Coutinho, A. J. D. Silvestre, *ChemSusChem* **2020**, *13*, 784–790.

[19] L. Miliander, *Pulp Washing*, **2009**.

[20] J. Wildschut, A. T. Smit, J. H. Reith, W. J. J. Huijgen, *Bioresour. Technol.* **2013**, *135*, 58–66.

[21] M. Wu, D. Zhao, J. Pang, X. Zhang, M. Li, F. Xu, R. Sun, *Ind. Crops Prod.* **2015**, *66*, 123–130.

[22] O. Hahlbohm, *The "Two Team Project,"* **2013**.

[23] S. Khandelwal, Y. K. Tailor, M. Kumar, *J. Mol. Liq.* **2016**, *215*, 345–386.

[24] A. Paiva, R. Craveiro, I. Aroso, M. Martins, R. L. Reis, A. R. C. Duarte, *ACS Sustain. Chem. Eng.* **2014**, *2*, 1063–1071.

[25] C. Alvarez-Vasco, R. Ma, M. Quintero, M. Guo, S. Geleynse, K. K. Ramasamy, M. Wolcott, X. Zhang, *Green Chem.* **2016**, *18*, 5133–5141.

[26] X. J. Shen, J. L. Wen, Q. Q. Mei, X. Chen, D. Sun, T. Q. Yuan, R. C. Sun, *Green Chem.* **2019**, *21*, 275–283.

[27] M. Francisco, A. Van Den Bruinhorst, M. C. Kroon, *Green Chem.* **2012**, *14*, 2153–2157.

[28] J. G. Lynam, N. Kumar, M. J. Wong, *Bioresour. Technol.* **2017**, *238*, 684–689.

[29] A. K. Kumar, B. S. Parikh, M. Pravakar, *Environ. Sci. Pollut. Res.* **2016**, *23*, 9265–9275.

[30] C. W. Zhang, S. Q. Xia, P. S. Ma, *Bioresour. Technol.* **2016**, *219*, 1–5.

[31] Z. Chen, C. Wan, *Bioresour. Technol.* **2018**, *250*, 532–537.

[32] J. L. K. Mamilla, U. Novak, M. Grilc, B. Likozar, *Biomass and Bioenergy* **2019**, *120*, 417–425.

[33] Y. Chen, L. Zhang, J. Yu, Y. Lu, B. Jiang, Y. Fan, Z. Wang, *R. Soc. Open Sci.* **2019**, *6*, 181757.

[34] A. M. Da Costa Lopes, J. R. B. Gomes, J. A. P. Coutinho, A. J. D. Silvestre, *Green Chem.*

2020, *22*, 2474–2487.

[35] E. S. Morais, P. V. Mendonça, J. F. J. Coelho, M. G. Freire, C. S. R. Freire, J. A. P. Coutinho, A. J. D. Silvestre, *ChemSusChem* **2018**, *11*, 753–762.

[36] L. X. Zhang, H. Yu, H. B. Yu, Z. Chen, L. Yang, *Chinese Chem. Lett.* **2014**, *25*, 1132–1136.

[37] E. Erbas Kiziltas, A. Kiziltas, M. Blumentritt, D. J. Gardner, *Carbohydr. Polym.* **2015**, *129*, 148–155.

[38] a. Sluiter, B. Hames, R. Ruiz, C. Scarlata, J. Sluiter, D. Templeton, D. Crocker, *NREL/TP-510-42618 Analytical Procedure - Determination of Structural Carbohydrates and Lignin in Biomass*, **2012**.

[39] D. Queiros, C. Rangel, P. C. Lemos, S. Rossetti, *Fermentation* **2018**, *4*, 1–16.

[40] J. Li, Y. Xu, M. Zhang, D. Wang, *Energy and Fuels* **2017**, *31*, 13769–13774.

[41] T. Rosenau, A. Potthast, N. S. Zwirchmayr, H. Hettegger, F. Plasser, T. Hosoya, M. Bacher, K. Krainz, T. Dietz, *Cellulose* **2017**, *24*, 3671–3687.

[42] I. Forsskåhl, H. Tylli, C. Olkkonen, *J. Pulp Pap. Sci.* **2000**, *26*, 245–249.

[43] D. Gaspar, S. N. Fernandes, A. G. De Oliveira, J. G. Fernandes, P. Grey, R. V. Pontes, L. Pereira, R. Martins, M. H. Godinho, E. Fortunato, *Nanotechnology* **2014**, *25*, 1–11.

[44] B. W. Chieng, N. A. Ibrahim, W. M. Z. W. Yunus, M. Z. Hussein, *Polymers (Basel).* **2014**, *6*, 93–104.

[45] H. Kono, S. Yunoki, T. Shikano, M. Fujiwara, *J. Am. Chem. Soc.* **2002**, *124*, 7506–7511.

[46] S. Spinella, G. Lo Re, B. Liu, J. Dorgan, Y. Habibi, P. Leclère, J. M. Raquez, P. Dubois, R. A. Gross, *Polymer (Guildf).* **2015**, *65*, 9–17.

[47] R. Karinen, K. Vilonen, M. Niemelä, *ChemSusChem* **2011**, *4*, 1002–1016.

[48] R. Sun, J. Fang, P. Rowlands, *Polym. J.* **1998**, *30*, 289–294.

[49] F. Peng, J. L. Ren, F. Xu, J. Bian, P. Peng, R. C. Sun, *J. Agric. Food Chem.* **2010**, *58*, 1768–1776.

[50] X. Zhang, H. Wang, C. Liu, A. Zhang, J. Ren, *Sci. Rep.* **2017**, *7*, 1–10.

[51] R. Weingarten, J. Cho, W. C. Conner, G. W. Huber, *Green Chem.* **2010**, *12*, 1423–1429.

[52] Z. Cheng, J. L. Everhart, G. Tsilomelekis, V. Nikolakis, B. Saha, D. G. Vlachos, *Green Chem.* **2018**, *20*, 997–1006.

[53] S. A. Lisboa, D. V. Evtuguin, P. Neto, *Holzforschung* **2007**, *6*, 478–482.

[54] B. Esteves, A. V. Marques, I. Domingos, H. Pereira, *Maderas Cienc. y Tecnol.* **2013**, *15*, 245–258.

[55] D. Smink, A. Juan, B. Schuur, S. R. A. Kersten, *Ind. Eng. Chem. Res.* **2019**, *58*, 16348–16357.

[56] Y. Wang, X. Wang, Y. Xie, K. Zhang, *Cellulose* **2018**, *25*, 3703–3731.

[57] P. Singla, R. Mehta, D. Berek, S. N. Upadhyay, *J. Macromol. Sci. Part A Pure Appl. Chem.* **2014**, *51*, 350–361.

[58] A. Păucean, D. C. Vodnar, V. Mureşan, F. Fetea, F. Ranga, S. M. Man, S. Muste, C. Socaciu, *Acta Aliment.* **2017**, *46*, 1–8.

[59] K. Yuniarto, Y. A. Purwanto, S. Purwanto, B. A. Welt, H. K. Purwadaria, T. C. Sunarti, in *AIP Conf. Proc.*, **2016**, pp. 1–6.